

# An innovative and eco-friendly modality for synthesis of highly fluorinated graphene by an acidic ionic liquid: Making of an efficacious vehicle for anti-cancer drug delivery

**Jahanshahi, Mohammadjavad; Kowsari, Elaheh; Haddadi-Asl, Vahid; Khoobi, Mehdi; Bazri, Behrouz; Aryafard, Meysam; Lee, Jong Hyun; Kadumudi, Firoz Babu; Talebian, Sepehr; Kamaly, Nazila**

*Total number of authors:*
12

*Published in:*
Applied Surface Science

*Link to article, DOI:*
10.1016/j.apsusc.2020.146071

*Publication date:*
2020

*Document Version*
Peer reviewed version

Applied Surface Science
Manuscript Draft

Manuscript Number: APSUSC-D-19-15740

Title: An innovative and eco-friendly modality for synthesis of highly fluorinated graphene by ionic liquid: Making of an efficacious vehicle for anti-cancer drug delivery

Article Type: Full Length Article

Keywords: Eco-friendly synthesis; Fluorinated graphene; mild-temperature fluorination; Ionic liquid; Curcumin loading efficiency; Cancer drug delivery

Abstract: Fluorination of graphene has multitude merits owing to the peculiar temperament of the carbon-fluorine (C-F) bond. the Current synthesis modalities of fluorinated graphene (FG) is based on the usage of toxic materials at high temperature, which is problematic to be used. The methods to overcome these problems is challenging for chemists. Ionic liquids (ILs) have been used in several chemical processes as auxiliaries and eco-friendly alternative instead of volatile organic solvents (VOS) because of their properties. Consequently, herein we exploited a highly effective and green process for the synthesis of FG at mild temperature (80 °C), by using ammonium fluoride salt as fluorine agent, and a synthesized acidic IL ([TEA]+[TFA]-) as catalyst and co-solvent. Our goal was synthesis enriched FG with a high degree of fluorination (70.4 wt.% of F) and F/C ratio (2.4), which measured and confirmed by XPS analysis. Subsequently, the obtained FG was used as a nanocarrier for delivery of curcumin (Cur- a natural antitumor drug) to cancerous cells. The in-vitro results showed that these nanosheets possessed a higher Cur-loading efficiency (78.43%) when compared to FG that was purchased from industry (52.12%). This, in turn, translated into in-vitro anti-cancer effect when tested against cancerous cells (PC-3 cells).

# An innovative and eco-friendly modality for synthesis of highly fluorinated graphene by ionic liquid: Making of an efficacious vehicle for anti-cancer drug delivery

Mohammadjavad Jahanshahi, Elaheh Kowsari*, Vahid Haddadi-Asl, Mehdi Khoobi, Behrouz Bazri, Meysam Aryafard, Jong Hyun Lee, Firoz Babu Kadumudi, Sepehr Talebian, Nazila Kamaly, Mehdi Mehrali and Alireza Dolatshahi-Pirouz

*Corresponding author: Tel: +989127642216. E-mail address: kowsarie@aut.ac.ir (Elaheh Kowsari).

## Highlights

- Simple and cost effective process used to synthesize highly fluorinated graphene.
- The synthetic route applied is safe and eco-friendly at mild temperature using the synthesized ionic liquid.
- The highly degree of fluorination on graphene oxide surfaces (70.4 wt.% of F) obtained by presented method.
- The FG nanosheets showed a higher curcumin-loading efficiency (78.43%) to deliver the anti-cancer drug.

# An innovative and eco-friendly modality for synthesis of highly fluorinated graphene by ionic liquid: Making of an efficacious vehicle for anti-cancer drug delivery

Mohammadjavad Jahanshahi, Elaheh Kowsari*, Vahid Haddadi-Asl, Mehdi Khoobi, Behrouz Bazri, Meysam Aryafard, Jong Hyun Lee, Firoz Babu Kadumudi, Sepehr Talebian, Nazila Kamaly, Mehdi Mehrali and Alireza Dolatshahi-Pirouz

**Corresponding author: Tel: +989127642216. E-mail address: kowsarie@aut.ac.ir (Elaheh Kowsari).*

## Graphical abstract

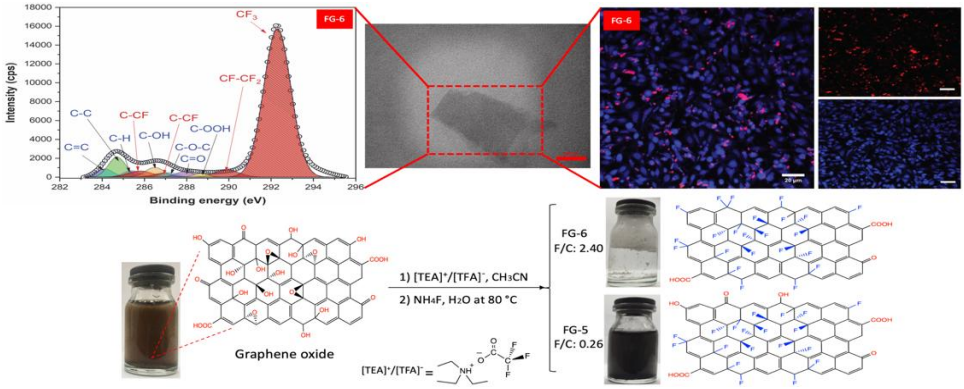

# An innovative and eco-friendly modality for synthesis of highly fluorinated graphene by ionic liquid: Making of an efficacious vehicle for anti-cancer drug delivery

Mohammadjavad Jahanshahi[a], Elaheh Kowsari*[a], Vahid Haddadi-Asl[b], Mehdi Khoobi[c], Behrouz Bazri[a], Meysam Aryafard[d], Jong Hyun Lee[e], Firoz Babu Kadumudi[f], Sepehr Talebian[g,h], Nazila Kamaly[e,i], Mehdi Mehrali[f] and Alireza Dolatshahi-Pirouz[f,j]

[a.] *Amirkabir University of Technology, Department of Chemistry, 1591634311 Tehran, Iran.*

[b.] *Amirkabir University of Technology, Department of Polymer Engineering and Color Technology, 1591634311 Tehran, Iran.*

[c.] *The Institute of Pharmaceutical Sciences (TIPS), Tehran University of Medical Sciences, 1417614411, Tehran, Iran.*

[d.] *University of South Bohemia, Faculty of Science, Branišovská 1760, 37005 České Budějovice, Czech Republic.*

[e.] *Technical University of Denmark, Department of Micro and Nanotechnology, DTU Nanotech, Bioinspired Nanomaterials Lab, 2800, Kgs, Lyngby, Denmark.*

[f.] *Technical University of Denmark, Department of Health Technology, Center for Intestinal Absorption and Transport of Biopharmaceuticals, 2800, Kgs, Lyngby, Denmark.*

[g.] *University of Wollongong, Illawarra Health and Medical Research Institute, NSW 2522, Australia.*

[h.] *University of Wollongong, Intelligent Polymer Research Institute, ARC Centre of Excellence for Electromaterials Science, AIIM Facility, NSW 2522, Australia.*

[i.] *Imperial College London, Department of Chemistry, Molecular Science Research Hub, W12 0BZ, London, UK.*

[j.] *Radboud university medical center, Radboud Institute for Molecular Life Sciences, Department of Dentistry-Regenerative Biomaterials, Philips van Leydenlaan 25, 6525EX Nijmegen, The Netherlands.*

*Corresponding author: Tel: +989127642216. E-mail address: kowsarie@aut.ac.ir (Elaheh Kowsari).*

**Abstract**

Fluorination of graphene has multitude merits owing to the peculiar temperament of the carbon-fluorine (C-F) bond. the Current synthesis modalities of fluorinated graphene (FG) is based on the usage of toxic materials at high temperature, which is problematic to be used. The methods to overcome these problems is challenging for chemists. Ionic liquids (ILs) have been used in several chemical processes as auxiliaries and eco-friendly alternative instead of volatile organic solvents (VOS) because of their properties. Consequently, herein we exploited a highly effective and green process for the synthesis of FG at mild temperature (80 °C), by using ammonium fluoride salt as fluorine agent, and a synthesized acidic IL ([TEA]+[TFA]–) as catalyst and co-solvent. Our goal was synthesis enriched FG with a high degree of fluorination (70.4 wt.% of F) and F/C ratio (2.4), which measured and confirmed by XPS analysis. Subsequently, the obtained FG was used as a nanocarrier for delivery of curcumin (Cur- a natural antitumor drug) to cancerous cells. The in-vitro results showed that these nanosheets possessed a higher Cur-loading efficiency (78.43%) when compared to FG that was purchased from industry (52.12%). This, in turn, translated into in-vitro anti-cancer effect when tested against cancerous cells (PC-3 cells).

**Keywords:** Eco-friendly synthesis; Fluorinated graphene; mild-temperature fluorination; Ionic liquid; Curcumin loading efficiency; Cancer drug delivery

## 1. Introduction

The emergence of graphene back in 2004 initiated a powerful movement in two-dimensional nanomaterials research that took the world by storm[1]. Along these lines, graphene-based nanomaterials gained remarkable attention in nanotechnology predominantly owing to their peculiar nature including wide surface area (2600 $m^2\ g^{-1}$), exceptional conductor of electricity (2.50 × 105 $cm^2\ V^{-1}\ s^{-1}$) and heat (3000 $W\ m^{-1}\ K^{-1}$), and high optical transmittance (~ 97.7%)[2]. Despite all these advantages, unmodified graphene possesses a zero band gap along with inertness to reaction, which can further hinder the application of this nanomaterial in specific fields[3]. Consequently, functionalization of graphene (and its

derivatives) with organic or inorganic molecules emerged as a potential pathway to address the above-mentioned shortcomings. In line with this, fluorinated graphene (FG) emerged as inestimable graphene derivatives mainly on account of its distinguished properties such as superhydrophobicity, low surface energy, excellent chemical and thermal stabilities, and wideband gap[4,5]. The fluorinated graphene is comprised of fluorine (F) atoms that were existing in the form of C-F covalent bonds coincided with structural transformation of C-C bonds from $sp^2$ to $sp^3$ formation[6]. Recently, much efforts have been made towards controlling the C-F bonding characters, F/C ratios, and configuration of fluorinated graphene, as these parameters play a substantial role in determining some of the essential properties of FG including its band gap, stability, electrical and thermal conductivity, and dispersibility[4]. Along similar veins, the methods for synthesizing fluorinated graphene, which has been cited in a few reports, are generally categorized into two groups: (I) Exfoliation methods that include thermal exfoliation[7,8], modified Hummer's exfoliation[9], and sonochemical exfoliation[10], all of which employ the commercially available graphite fluoride (GrF) powders along with severe reaction conditions, that could inevitably destroy a portion of C-F bonds in the fluorinated graphene[11]. (II) Direct graphene fluorination method which has been achieved through utilizing a variety of reactions such as fluorination gas[12,13], plasma fluorination[14], photochemical/electrochemical synthesis[15], and hydrothermal fluorination[16–20], all of which require high thermal treatment temperature and yield a low F content[21]. Therefore, the progress of a safe, secure, low-cost, and effective synthesis route of FG with adaptive F/C atomic ratio is of high demand. For instance, inspired by hydrothermal process principles, Z Wang et al. synthesized FG through a simple hydrothermal reaction including homogeneously dispersed GO in the presence of hydrofluoric acid (HF)[6]. However, intrinsic disadvantages such as a highly corrosive fluorine agent (HF), high-temperature treatment (180 °C), special equipment for material handling, low F/C atomic ratios (from 0.1 to 0.48), and the toxic-fluorination sources were unavoidable in this procedure. Therefore, it was found that a solid fluorine source (as opposed to fluorine gas or volatile liquid sources) could potentially reduce the chemical hazards associated with the experiments, however,

solid fluorine sources have a low reactivity of the fluorination which can further jeopardize the efficiency of the reaction[22]. To this end, ionic liquids (ILs), which are categorized as organic salts, gained a foothold in various chemical processes owing to their unique features such as wide electrochemical window, high thermal stability and solvation capacity, as well as the high ionic conductivity with low vapor pressure at the surface [23–27]. Features of ILs depend on choosing the cations and anions that are used in the structure of ILs[25,28–30]. Triethylammonium trifluoroacetate ($[TEA]^+[TFA]^-$) as an acidic ionic liquid, was synthesized to have a catalysis role in fluorination of graphene oxide. More specifically, acidic ionic liquid allows larger protonation of hydroxyl and epoxide groups, which can subsequently increase the fluorination efficiently of this reaction.

In this work, we present a highly effective and eco-friendly method for the synthesis of FG at a mild temperature (80 °C) using ammonium fluoride salt as fluorine agent and a synthesized acidic ionic liquid ($[TEA]^+[TFA]^-$). We have specifically used a mixed solvent system comprised of ionic liquid, acetonitrile, and water. Water was used since it has better solubility for ammonium fluoride ($NH_4F$) compare to other components, and it also increases the number of fluoride anions in the solution which could be beneficial for fluorinating of graphene oxide. The ionic liquid-water system not only could significantly enhance the reactivity of $NH_4F$ salt, but it could also introduce efficient energy consumption and minimize the costs while reducing the risk of any unforeseen chemical accidents. To date, the obtained FG of our procedure, among mild temperature methods, has the highest degree of fluorination (70.4 wt% of F) and F/C ratio (2.4), which measured and confirmed by XPS analysis. Fluorine to carbon ratios (F/C ratio) of the synthesized samples prepared by different fluorination routes are presented in Table 1. Most remarkably, owing to attractive properties of the obtained fluorinated graphene including significant electronegativity difference between carbon and fluorine, and the high polarity of the C–F bonds, we have explored the application of this compound for cancer drug delivery. Accordingly, FG was further loaded with curcumin (Cur) as a natural antitumor drug and characterized as a nanocarrier for anti-cancer drug delivery. Most remarkably, the obtained results showed that the FG synthesized in this work

(FG-6@Cur) possessed a higher Cur loading efficiency (78.43%) when compared to that of FG that was purchased from Sigma-Aldrich (52.12%), possibly due to more π–π* stacking interaction and the more hydrophobic interaction between highly hydrophobic structures of our FG and hydrophobic nature of curcumin. Overall, our proposed synthesis route represents an exciting alternative to the already established methods, as it provides a safe, secure, and highly efficient modality to synthesize biocompatible FG with a high F/C ratio, which to this date is unprecedented among mild temperature methods. Finally, FG-6@Cur was introduced to higher Cur loading efficiency and the ensuing anti-cancer effect.

**Table 1.** Comparison of synthesis methods, preparation conditions, and F/C ratios of fluorinated graphene

| Method types | Method names | Graphene-based materials | Fluorine agents | Oxidizing agents | Solvents | F/C ratios | Temp. | Time | Year | Ref. |
|---|---|---|---|---|---|---|---|---|---|---|
| **Exfoliation** | Thermal | Fluorinated graphite | - | - | - | 0.05 | 650 °C | 6 h | 2018 | [7] |
| | | Fluorinated graphite | - | NaOH, KOH | $H_2SO_4$:$HNO_3$ | 0.22-0.37 | 200 °C | 10 h | 2015 | [8] |
| | Hummers | Fluorinated graphite | - | $KMnO_4$ | $H_3PO_4$:$H_2SO_4$ | 0.07-0.36 | 90 °C | 12 h | 2013 | [9] |
| | Solvothermal | Fluorinated graphite | - | - | $CHCl_3$ or $CH_3CN$ | 0.9 | 150 °C-RT | 10+6 h | 2014 | [10] |
| **Directly fluorination** | Plasma fluorination | CVD Monolayer graphene | SF6 plasma | - | - | 0.05-0.32 | RT | 10 s-90 s | 2016 | [14] |
| | Gas fluorination | Monolayer graphene | $XeF_2$ | - | - | 0.5-0.9 | RT | 0.5 -10 min | 2019 | [12] |
| | | GO | $F_2$ | - | - | 0.08-0.23 | 200 °C | 1 h | 2019 | [13] |
| | Photochemical synthesis | GOQDs | $XeF_2$ | - | - | 0.28-1.44 | RT | 10 min | 2019 | [15] |
| | Hydrothermal fluorination | GO dispersion | HF (40 wt%) | - | - | 0.1-0.48 | 180 °C | 30 h | 2012 | [16] |
| | | GO dispersion | HF (40 wt%) | - | - | 0-0.05 | 90-180 °C | 24 h | 2016 | [17] |
| | | GO dispersion | HF (40 wt%) | - | $HNO_3$ | 0.05-0.23 | 160 °C | 12 h | 2019 | [18] |
| | | GO dispersion | DAST | - | $C_6H_4Cl_2$ | 0.39 | RT | 3 days | 2014 | [19] |
| | | Graphite oxide | XtalFluor-E and $Et_3N.3HF$ | - | $CH_2Cl_2$ | 0.01-0.07 | 25-40 °C | 22 h | 2018 | [20] |
| **This study** | Mild temperature fluorination | Graphene oxide | $NH_4F$ | - | IL[1], $CH_3CN$, and $H_2O$ | 0.26-2.4 | 80 °C | 48 h | - | - |

[1] **IL: $[TEA]^+/[TFA]^-$**

## 2. EXPERIMENTAL

### 2.1. Materials

C2C12 cell lines were obtained from the American Type Culture Collection (ATCC), and Buffer RLT (lysis buffer) prepared from a Qiagen kit. RPMI-1640 Medium, 1% Penicillin-Streptomycin, Fetal bovine serum (FBS), Dulbecco's modified Eagle's medium (DMEM), Trypsin-EDTA solution, Phosphate buffered saline (PBS), graphite flakes, Fluorinated graphite polymer, Trifluoroacetic acid (TFA), Chloroform, Trimethylamine (TEA), Ammonium fluoride ($NH_4F$), acetonitrile (MeCN), dichloromethane, Cell Counting Kit-8 (CCK-8) and other reagents provided from Sigma-Aldrich without any further purification.

### 2.2. Instruments and Measurements

UV-Vis spectroscopy analysis was conducted using a Shimadzu UV-2600 (Japan)), and was also read by a Tecan Spark 20M multimode microplate reader (Switzerland). The FTIR spectra were collected using a PerkinElmer Spectrum 100 FTIR spectrometer (USA) with the scan range of 400-4000 $cm^{-1}$ recording 16 scans at a resolution of 4 $cm^{-1}$. The $^{1}H$ NMR spectra were performed at room temperature on a Varian Mercury 400 MHz Spectrometer (USA). X-ray photoelectron spectroscopy (XPS) measurements were investigated by an Escalab 220i-XL from Thermo Scientific, using a monochromatic Al Kα X-ray source with a photon energy of 1486.7 eV. The average lateral size distribution of all samples, nanoparticles morphology and dimensions examinations were performed by a field emission-scanning electron microscopy (FESEM, Tescan Mira) equipped with an energy dispersive spectroscopy (EDS) and a Philips EM208S transmission electron microscopy (TEM) with an accelerating voltage of 100 kV. The material thickness and size were measured using a tapping mode of Park NX20 Atomic Force Microscopy (South Korea).

### 2.3. Synthesis of Triethylammonium-Trifluoroacetate $[TEA]^+[TFA]^-$

About 18 g of trimethylamine (TEA) was dispersed in 50 ml of dichloromethane solvent. The solution was mixed for 1 hour at room temperature. Trifluoroacetic acid (25.5 g, 16 ml) was dropped into the triethylamine solution in an ice bath for 3 hours. After the addition of trifluoroacetic acid, the reaction solution was stirred at room temperature for an additional period of 5 hours to ensure the reaction proceeded to completion. Finally, the excess amount of trifluoroacetic acid and the traces of dichloromethane were evaporated in high vacuum at 90 °C until the constant weight of the residue obtained. The yield of $[TEA]^+[TFA]^-$ was 97% (42.5 g).

### 2.4. Synthesis of the graphene oxide (GO)

Graphite flakes used as a source to synthesize GO nanosheets through the improved hummers' method[31]. About 3 g of graphite flakes were dispersed in a 9:1 mixture of concentrated $H_2SO_4$:$H_3PO_4$ (360:40 mL) and stirred for 1 h. An aliquot 18 g of $KMnO_4$ was then added to the mixture and stirred at 50 $^{\circ}$C for 24 h. Then, the mixture was cooled by pouring onto a mixture of 400 mL ice-water with 5 mL $H_2O_2$ (30%). The final product had a yellowish-brown color. The dispersion was left to precipitate, and the supernatant separated overnight and decanted away. The solid product was then washed in sequence with 200 mL of 30 wt. % HCl and 200 mL of ethanol for each wash then filtered over a PTFE membrane (0.45 µm pore size) and saturated in diethyl ether. Finally, about 200 mL of water was added to the resulting GO precipitate and sonicated adequately with a probe-sonicator for about 3 h to obtain an exfoliated GO nanosheet.

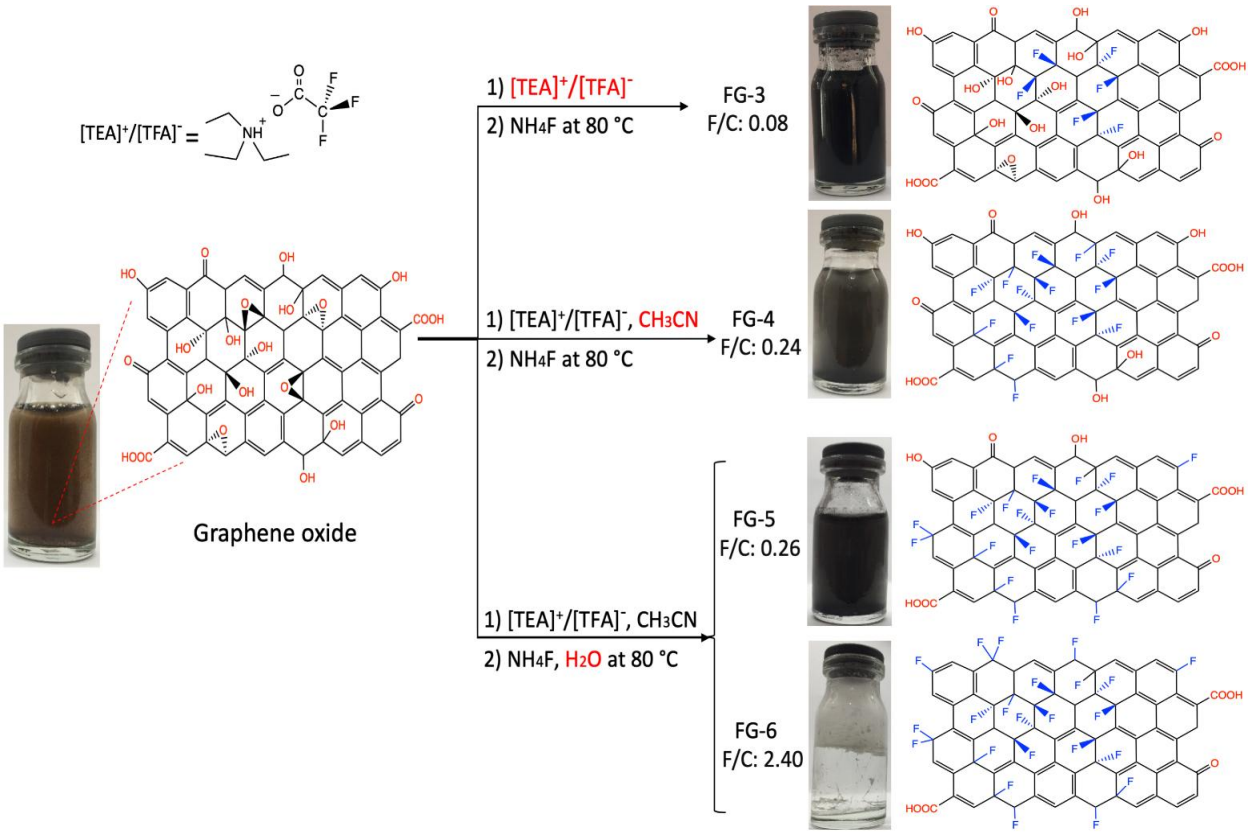


**Figure 1**. The schematic illustration of the synthesis condition and photographs of GO, and all FG that synthesized.

### 2.5. Synthesis and characterizations of fluorinated graphene sheets

Fluorinated graphene samples were synthesized using either of the two different procedures: hydrothermal method (high-temperature method), and mild temperature fluorination method using the ionic liquid. For synthesizing FG-2 sample with the hydrothermal method, 50 mL of GO dispersion (2 mg/mL in NMP) and 6 mL HF was mixed for 10 min in an ultrasonic bath. Then, the solution was moved into a 50 mL Teflon-lined autoclave and kept at 180 °C for 30 h. The autoclave let to be cooled typically to room temperature after the process. Lastly, the microporous membrane used to collect the product by filtration. The separated product washed thoroughly with ultrapure water and then dried through freeze-drying. For synthesizing FG samples with the mild temperature fluorination method using ionic liquid, 100 mg of GO was dispersed in 8 mL of $[TEA]^{+}[TFA]^{-}$ and 500 mg of $NH_4F$ was dispersed in acetonitrile, and then

the two mixtures were mixed for 30 min by ultrasonication. Thusly, the solution was moved into a 100 mL Teflon round bottom flask and refluxed at 80 °C for 48 h. Finally, the FG sheets precipitate was decanted from the flask and then centrifuged at 13000 rpm for 1 h and washed with Milli-Q water several times to remove the by-product. The final powder was dried through freeze-drying, and sample FG-4 was obtained. In addition, FG-3 sample was synthesized by the same procedure of FG-4 sample except a lack of acetonitrile as solvent. For more evaluation, FG-5 sample was also prepared which is the same as that of above with an excess amount of water. Simultaneously, a fluffy white hydrophobic phase at the top of the flask was observed to precipitate out of solution and was named FG-6, whereas the black phase settled down in solution which termed FG-5. The two phases were allowed to be separated overnight, after which both FG-5 and FG-6 samples had formed, as pictured in Figure 1. The final product FG sheets were characterized by Energy-dispersive X-ray spectroscopy (EDX) and the synthesis methods are summarized in Table 2, and for comparison, fluorinated graphene purchased of Sigma-Aldrich (FG-1) was exploited.

**Table 2.** Elemental composition of GO, FG-1 and all FG that synthesized at the different conditions and measured by EDX spectra.

| Entry | Fluoride Source | Solvent | $H_2O$ (mL) | $[TEA]^+[TFA]^-$ (mL) | Reaction condition | | Oxygen (Wt. %) | Fluorine (Wt. %) | F/C ratio |
|---|---|---|---|---|---|---|---|---|---|
| | | | | | Temp.(°C) | Time(h) | | | |
| **GO** | - | - | - | - | - | - | 42.1 | 0 | 0 |
| **FG-1** | FG Sigma | - | - | - | - | - | - | 58.63 | 1.5 |
| **FG-2** | HF (6 mL) | NMP | - | - | 180 | 30 | 24.06 | 0.88 | 0.01 |
| **FG-3** | $NH_4F$ (0.5 g) | - | - | 8 | 80 | 48 | 14.22 | 2.17 | 0.03 |
| **FG-4** | $NH_4F$ (0.5 g) | MeCN | - | 8 | 80 | 48 | 22.30 | 16.68 | 0.31 |
| **FG-5** | $NH_4F$ (0.5 g) | MeCN | 5 | 8 | 80 | 48 | 17.91 | 26.56 | 0.51 |
| **FG-6** | $NH_4F$ (0.5 g) | MeCN | 5 | 8 | 80 | 48 | 1.9 | 53.1 | 1.18 |

### 2.6. Preparation of Curcumin loaded FG-1 and FG-6 nanocarriers

To prepare curcumin loaded FG-1 and FG-6 nanocarriers, 150 μg of each and 1000 μg of curcumin were dissolved in 2 mL DMSO/DI water (1:1) solution and mixed on a shaker for 20 h at 150 rpm. The obtained solution was centrifuged and separated two times at 13,000 rpm for 30 min. The amount of excess curcumin in the solution was specified by UV-Vis spectroscopy in the supernatant. The whole procedure was performed in dark conditions and measured three times. A calibration curve initially evaluated for quantification analysis using curcumin at different concentration in the DMSO/DI water (1:1) solution was generated. The loading efficiency (LE) and loading content (LC) of curcumin in nanocarriers were calculated according to the following equations[32,33]:

$$\text{LE (\%)} = \frac{\textbf{amount of drug loaded}}{\textbf{amount of drug loaded+polymer}} \times 100 \quad \text{Eq. (A.1)}$$

$$\text{LC (\%)} = \frac{\textbf{amount of drug loaded}}{\textbf{Total polymer amount}} \times 100 \quad \text{Eq. (A.2)}$$

### 2.7. Cell viability and cytotoxicity assay

The cytotoxicity of FG nanocarrier and cell viability of FG-Cur complex besides Free-Cur was evaluated by a colorimetric cell counting kit (CCK-8). PC3 cells (prostate cancer cells) were seeded in 96-well plates at a density of 5000 cells per well in 100 μL of DMEM media supplemented with 10% fetal bovine serum (FBS), penicillin-streptomycin (1%) and cultured for 24 h in the presence of in CO2 incubator (5% CO2) at 37 °C [34]. In addition, PC-3 cell lines were treated with 100 μL of fresh culture media containing FG, Free-Cur, and FG-Cur samples. After 24 h incubation at various FG concentrations and Cur concentrations of Free-Cur, and FG-

Cur samples, the cells were washed three times with fresh PBS solution and then 100 µL of culture medium containing 10% CCK8 solution was added to the cells and kept for more 3 hours. The absorbance value of solutions was estimated at 450 nm with a Tecan Spark 20M multimode microplate reader (Switzerland) [35]. The results were shown as the percentage of viable cells over untreated cells (as control) and represented as mean ± SD based on six independent experiments.

### 2.8. Cellular uptake

The cellular uptake of the FG-Cur cargo in PC-3 cell nuclei was investigated by confocal laser scanning microscopy (CLSM). PC-3 cell lines were seeded on a glass slide placed in 6-well plate ($1\times10^5$ cells/well) and grown for 24h. The culture media was replaced by fresh DMEM containing FG-Cur cargo at a fixed curcumin concentration (200 µg $mL^{-1}$) for 12h. The cells were washed three times with cold PBS solution and fixed with paraformaldehyde (4% (v/v)) for 20 min at 37°C. The cell membranes were permeabilized with 300 µL of Triton X-100 in PBS solution (0.15% (v/v)) for 20 min and stained by 300 µL of DAPI solution (0.2 g $mL^{-1}$). Confocal fluorescence imaging was performed by using a 40 X objective lens (Nikon, Germany). The fluorescent probes consist of Curcumin and DAPI analyzed by ImageJ v1.52a [36,37].

### 2.9. Statistical analysis

Statistical analysis was measured using GraphPad Prism 6 software (USA). The data were represented as the means ± SD. The statistical significant differences between treatment groups or intracellular uptake efficiency of FPS-Cur complexes in three cancer cell lines were obtained through two-way analysis of variance (ANOVA), followed by Bonferroni's multiple comparisons test, respectively. The statistical significant difference was defined as *($P < 0.05$), **($P < 0.01$), ***($P < 0.001$) and ****($P < 0.0001$).

## 3. Results and discussion

### 3.1. Structural and compositional analysis

As shown in Figure S1, the purities of synthesized ionic liquid ($[TEA]^+[TFA]^-$) was corroborated by 1H and 13C NMR spectroscopies. The 1H NMR of $[TEA]^+[TFA]^-$ in $D_2O$ shows two peaks at ~1.18 ppm (t, 3H) and 3.10 (m, 2H). In addition, this ionic liquid displayed four distinguished signals at ~8, 46.6, 111.9_120.6 and ~162 ppm in their 13C NMR spectra. These signals originate from $–CH_3$, $–CH_2–$, $–CF_3$ and C=O bonds, respectively.

FT-IR analysis was used for the investigation of the chemical composition, and structures change of both before and after fluorination of GO. Figure 2 presents the FTIR spectra, where several characteristic peaks for GO and samples FG-2, FG-3, FG-4, FG-5 with various functional groups were observed: the broad transmittance band of OH stretching in the range 3100-3400 $cm^{-1}$, C=O stretching vibrations from carbonyl and carboxyl groups (1730 $cm^{-1}$), C=C stretching (1620 $cm^{-1}$), O-H bending vibrations from hydroxyl groups (1380 $cm^{-1}$), and alkoxy C-O stretching vibration (1050 $cm^{-1}$)[38–40]. However, after fluorination of GO, all samples had an additional wide band with a maximum ranging from 1150 to 1220 $cm^{-1}$, which can be ascribed to stretching vibrations of a change of the C–F bond nature from “semi-ionic” to “covalent type”[41]. As the fluorine content increases, a shift towards higher wavenumbers observed for the C-F vibration band. Accordingly, the intensity of the oxygen functional groups was decreased due to the formation of the C-F functional group in all FGO samples. However, it should be noted that in the case of samples FG-5 and FG-6, their structures involved one active C-F band centered at 1205 $cm^{-1}$ and the oxygen functional groups were absent, which is acceptably correspond with the sample FG-1 (Graphite Fluoride powder obtained of Sigma-

Aldrich (GrF)). This observation was strong evidence for successful fluorination of GO with high fluorine content.

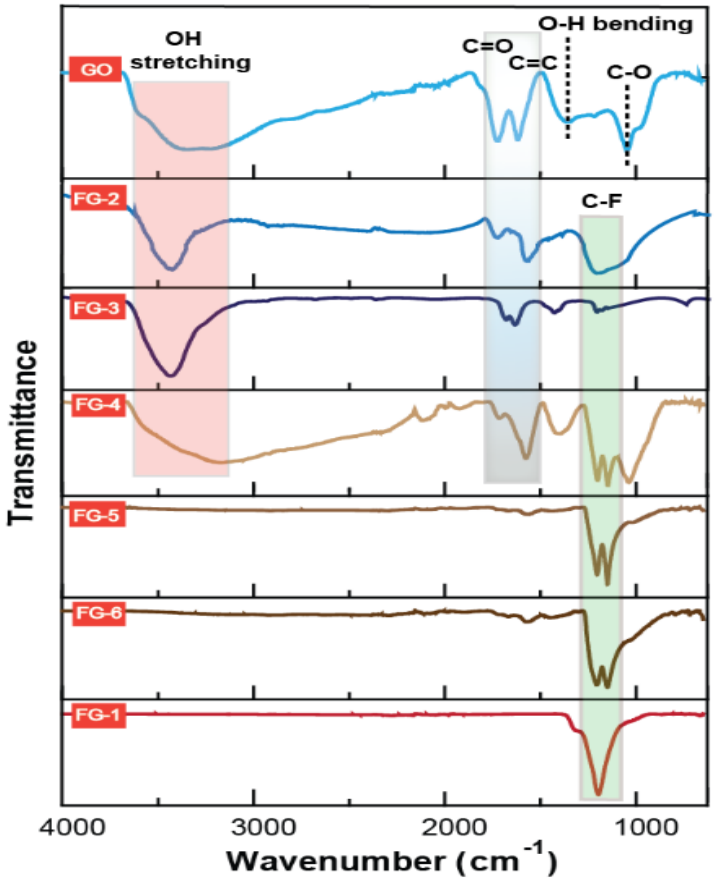


**Figure 2.** FTIR spectra of GO, FG-1 and all FG that synthesized.

Furthermore, the element distribution and concentration were measured by Energy-dispersive X-ray spectroscopy (EDS). The results for element distribution are shown in Figure 3a-c. As seen, fluorine distributed homogenously in all the fluorinated products. The composition of GO and all fluorinated samples were showed based on C, O, and F peak areas in Figure 3d and the calculated F/C ratios with the concentration of elements are summarized in Table 2. It can be found that the fluorine content rises using our method with ionic liquid at a mild temperature (80 °C) and indicates full fluorination of graphene with high F/C ratios between 0.51 and 1.2 for FG-5 and FG-6, respectively. While previous hydrothermal method exposed partial fluorination with

low F/C ratio (≈0.03) for FG-2. In addition, from Table 2 it is clearly evident that increasing the content of fluorine is related to the suppression of oxygen content. This designates fluorine favorably substitutes the remaining oxygen functionalities.

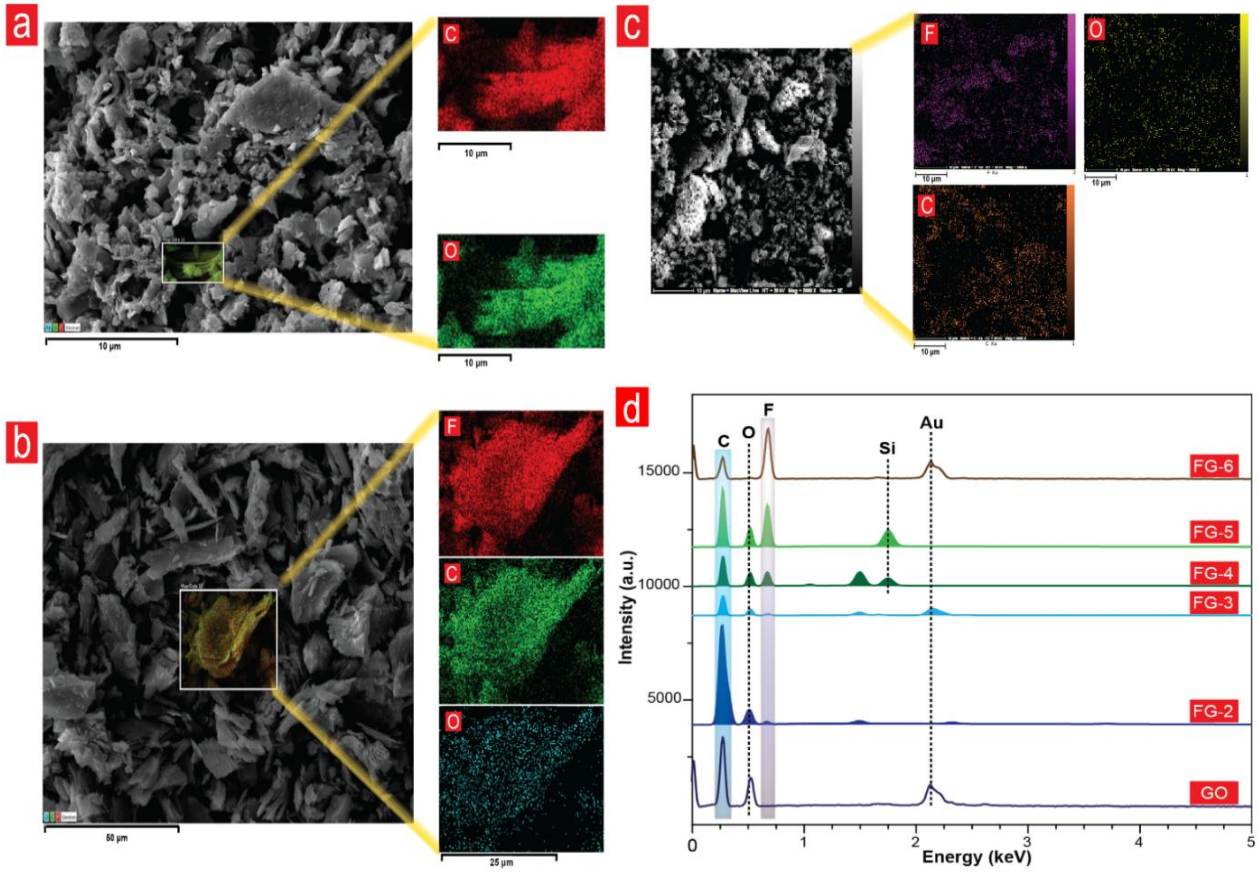


**Figure 3.** FESEM images and elemental mapping of GO (a), FG-6 (b), FG-5 (c) and EDX spectrums of the as-prepared GO, and all FG based on C, O, and F peak areas were showed (d).

Differences in the elemental concentration found between EDS and other elemental analysis (i.e. XPS) originate from the lower accuracy of EDS on non-planar samples. All the FG samples, along with GO have been investigated by XPS analysis to obtain F/C ratios. As seen in Figure 4, the significant role of suggested fluorination mechanism related to the oxygen-containing functions in GO sample. The elemental configuration and nature of the carbon chemical bonds found for GO and FG samples form XPS characterization. As seen, the oxygen-containing group

functions decreased drastically during the reduction process of fluorination reactions, and an apparent F1s functional peak appeared in FG samples. The presence of F1s functional peak in the $C1_S$ region confirms that fluorine has been attached to the carbon framework through the mild temperature reaction consuming ammonium fluoride salt as fluorine source and acidic ionic liquid ($[TEA]^+[TFA]^-$). Results from the fluorination of pristine GO for the C1s region reported for all FG samples. The C1s spectrum of GO was fitted for the functional groups as C-C ($sp^2$- 284.0–284.4 eV), C-C ($sp^3$- 284.5–284.9 eV), C-H (285.0–285.3 eV), C-OH (286.2–286.7 eV), C-O-C (286.8–287.3), C(O) (287.5–288 eV) and COOH in the range of (288.5–289 eV)[42]. As shown in Figure S2a, by converting GO into the FG samples, the content of oxygen decreases considerably, particularly for epoxy groups (C-O-C) showing the leading functional group for the fluorination mechanism of GO. After the addition of fluorine source, a new band appeared at ~286 eV, which ascribes to the C-F covalent bonds at the surface. The other bonds found in the FG samples were C-CF (285.8 eV) and C-$CF_2$ (286.9 eV), CF-$CF_2$ (289.9 eV), and C-$F_3$ (292.3 eV) (details are represented in Table 3) [16,43,44]. The relative content of fluorine and carbon from the high- resolution C1s spectra of the samples were measured to calculate the fluorination degree of the process (F/C ratio). Details are presented in Table 4. As calculated, the highest F/C ratio obtained for FG-6 sample as approximate 2.40. The obtained results indicating that the suggested fluorination process in this study to yield FG products in mild temperature process has the maximum degree of fluorination reported to date.

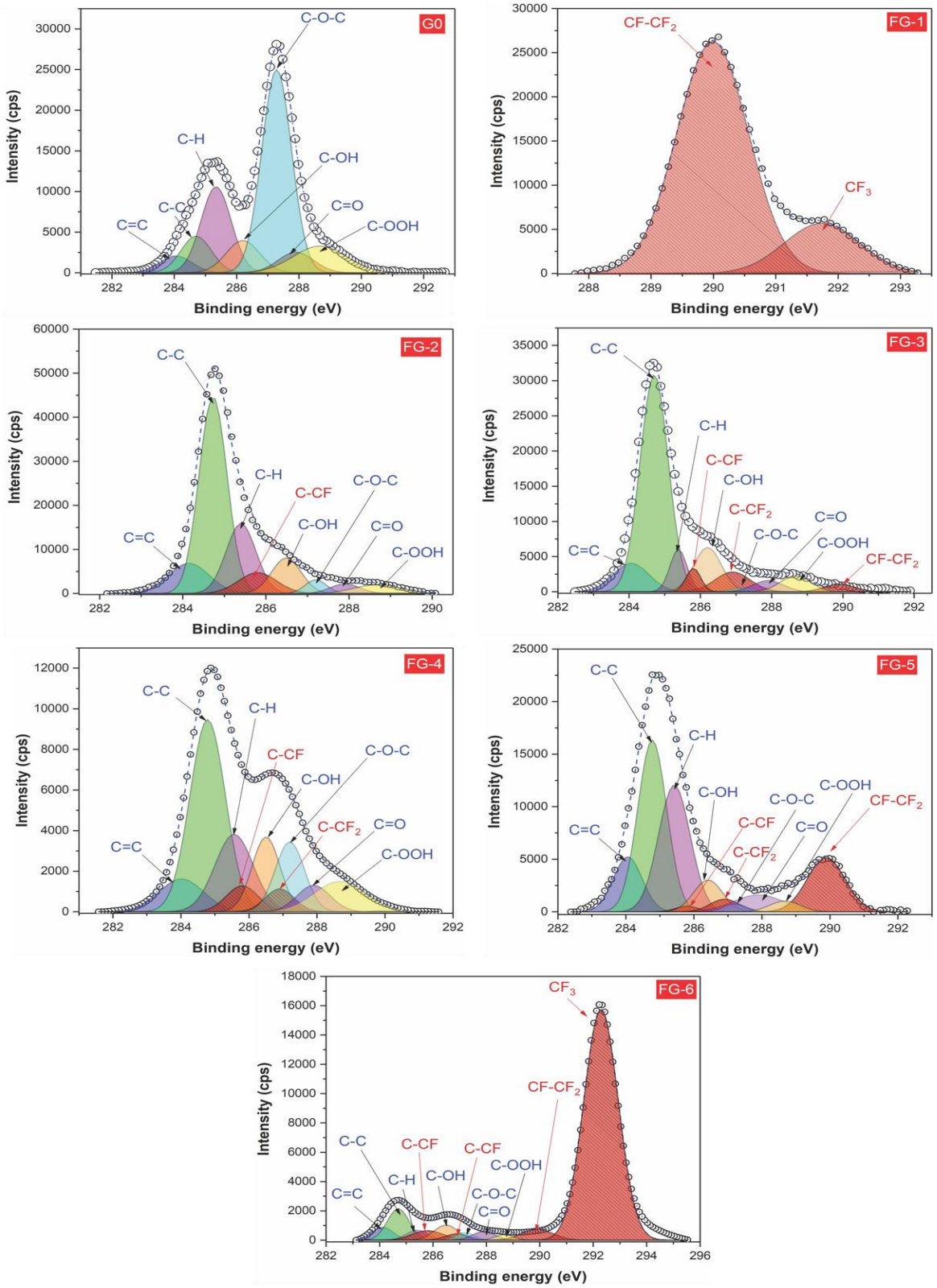


**Figure 4**. Deconvoluted XPS of the C1s core-level spectra of Go, FG-1 and all FG that synthesized with different F/C ratios.

**Table 3.** Ascription, location, and content (%) of fluorine-containing groups in the sample of FG-1 and all FG that synthesized with different F/C ratios.

| **Ascription** | | **C-CF** | **C-$CF_2$** | **CF-$CF_2$** | **$CF_3$** |
|---|---|---|---|---|---|
| **Location (eV)** | | **285.8** | **286.9** | **289.9** | **292.3** |
| **Samples and Content (%)** | **FG-1** | - | - | 81.4 | 18.6 |
| | **FG-2** | 6.3 | 0 | 8.0 | - |
| | **FG-3** | 3.1 | 6.1 | 2.0 | - |
| | **FG-4** | 4.3 | 3.4 | 0.2 | - |
| | **FG-5** | 0.8 | 2.4 | 13.3 | - |
| | **FG-6** | 2.8 | 1.4 | 3.3 | 73.7 |

**Table 4.** Elemental composition of GO, FG-1, and all FG that synthesized with different F/C ratios and measured by XPS survey spectra.

| **Samples** | **Oxygen** (wt.%) | **Carbon** (wt.%) | **Fluorine** (wt.%) | **F/C ratio** |
|---|---|---|---|---|
| **GO** | 33.5 | 66.5 | 0 | 0 |
| **FG-1** | 21.9 | 33.8 | 44.3 | 1.31 |
| **FG-2** | 19.7 | 78.8 | 1.5 | 0.02 |
| **FG-3** | 57.5 | 39.4 | 3.1 | 0.08 |
| **FG-4** | 50.3 | 40.4 | 9.9 | 0.24 |
| **FG-5** | 53.5 | 42.3 | 11.2 | 0.26 |
| **FG-6** | 0.3 | 29.3 | 70.4 | 2.40 |

The morphology and dimensions of graphene oxide and fluorinated graphene nanosheets were evaluated using field emission-scanning electron microscopy (FESEM). Accordingly, GO sheets possessed soft surface with multi-layer and large sheets (Figure 5a & 5b), but after the fluorination process, the FG-5 sample appeared ultrathin and crumpled fluorinated graphene nanosheets (Figure 5c). In addition, the high roughness and the thin layer sheets were observed for the FG-6 sheets (Figure 5d). Overall, FG samples showed a few layers, flexible sheet with nanometer roughness, wrinkled and folded edges.

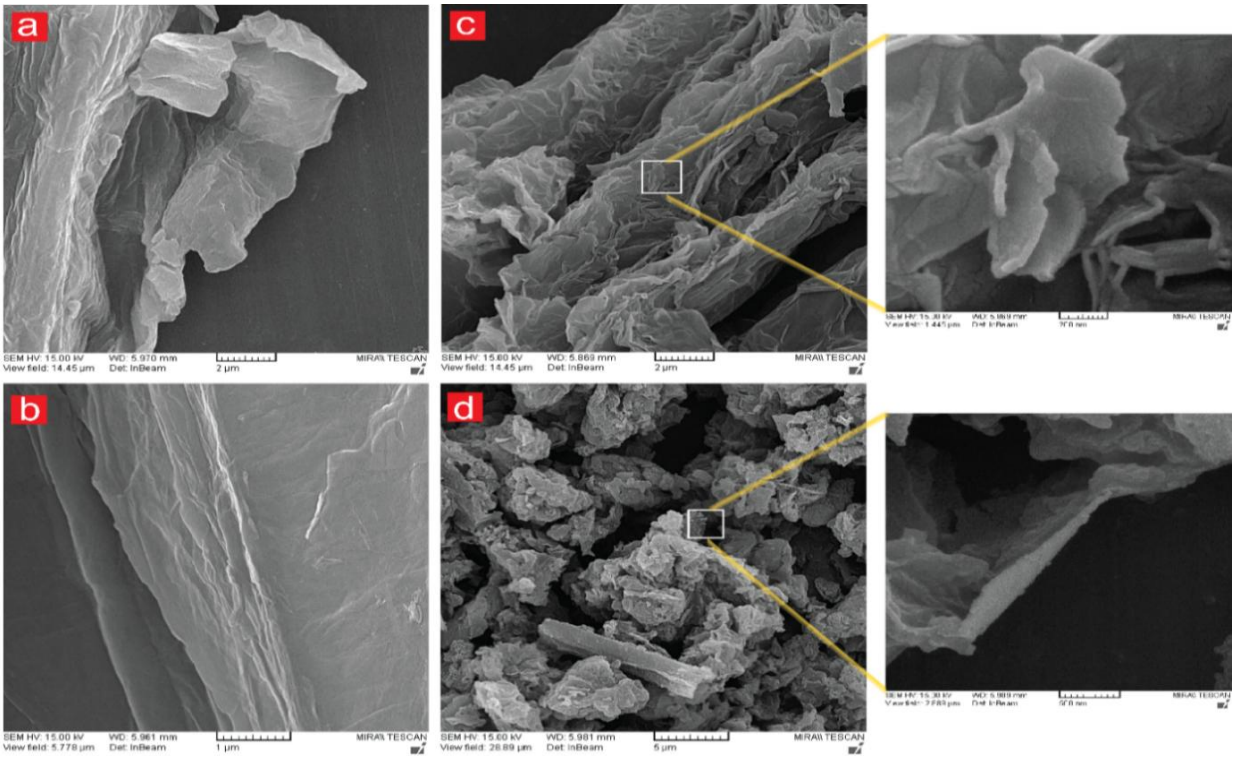


**Figure 5.** FESEM images of GO in different scale bars (a, b), FG-5 (c) and FG-6 (d).

TEM analysis also displayed that the FG-5 nanosheets had a transparent and flexible surface with wrinkled and folded edges(Figure 6a-b), indicating a high degree of exfoliation. As shown in Figure 6c-d, the FG-6 sample presented the thin layers and flexible sheets with regular surface. Identical surface-energy among the ionic liquid molecules and the GO sheets could be ascribed to the formation of thin layer fluorographene..

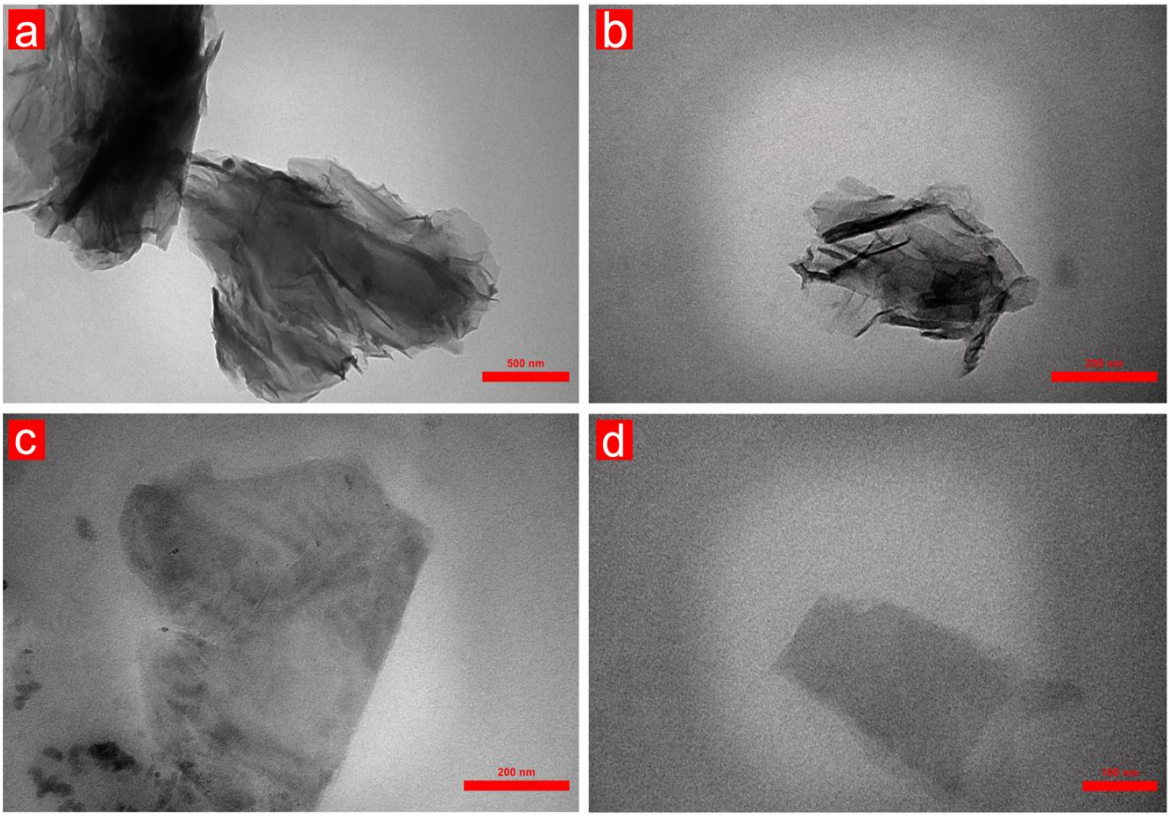


**Figure 6.** TEM images of FG-5 (a,b) and FG-6 nanosheets (c,d) in different scale bars.

Atomic Force Microscopy (AFM) was used to study the thickness and topography changes in FG-6 nanosheet[45]. As shown in Figure 2S.b, the AFM topography and height profiles of the FG-6 sheet revealed the thickness of 0.54–3.12 nm corresponds to 1–6 layers of the FG-6 sheet, and it agrees with the TEM images.

UV–Vis spectroscopy was conducted to understand chemical interactions in the composite samples (Figure 7b). The Free Cur-solution demonstrates a sharp absorption peak at 420 nm[46]. After loading of curcumin onto FG carrier, For FG-Cur sample, the characteristic absorption peak of Cur was observed at ≈434.5 nm, which indicating a red-shift due to the curcumin interaction with FG aromatic rings through a strong π–π* stacking interaction.

### 3.2. Loading capacity and efficiency studies

The amount of loading efficiency and drug loading content of curcumin in FG-1 and FG-6 samples were investigated at a fixed concentration of curcumin (1000 µg $mL^{-1}$) by UV–Vis analysis (Figure 7a). The average loading efficiency (LE) was calculated to be 52.12% for FG-1 and 78.43% for FG-6 nanocarrier. The calculations also showed that the average loading capacity (LC) was 25.38% for FG-6 per 150 µg of nanocarriers, which is three-fold more than FG-1 (LC= 8.20%). As seen, the FG-6 sample exhibited the highest potential for CUR loading in comparison to FG-1 that could be due to the more π–π* stacking interaction and the more hydrophobic interaction between highly hydrophobic structures of FG-6 and hydrophobic nature of curcumin.

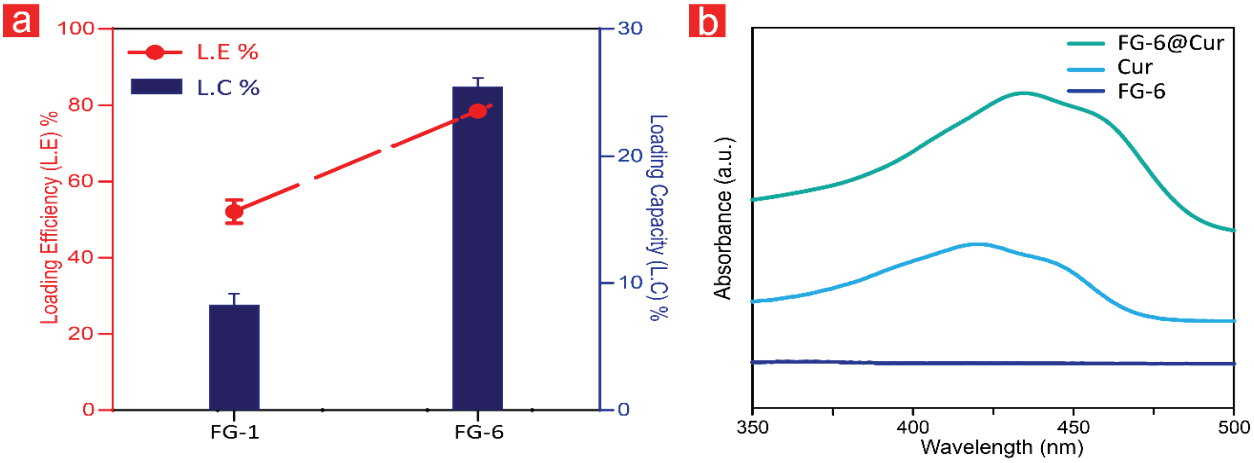


**Figure 7.** (a) Cur loading efficiency of FG-6 nanosheets as compared against that of FG-1 nanosheets (purchased from Sigma), and (b) UV-Vis spectroscopy of FG-6, Cur and Cur-loaded FG-6 nanosheets.

### 3.3. In Vitro biocompatibility of FG nanocarrier

For in vitro studies of FG-6 biocompatibility, a cytotoxicity test was implemented by a CCK-8 assay in the presence of FG-6 nanocarriers against PC-3 cells. As shown in Figures 8a, results showed a dose-dependent effect on cell viability. So that, FG-6 with very high dose (1000 µg $mL^{-1}$) displayed the lowest cell viability of the PC-3 cells (35.8%). While the viability of the PC-

3 cells was around 70% after 24h incubation at high dose of FG-6 (500 µg $mL^{-1}$). This illustrates that the synthesized FG-6 nanocarriers have no regular cell-killing activity, and the half-maximal inhibitory concentration ($IC_{50}$) values of FG-6 nanocarriers represent a very high dose (715.52 µg $mL^{-1}$) against the PC-3 cell lines. Obtained results suggest an excellent cytocompatibility for FG-6 nanocarriers in the range of 100-500 µg $mL^{-1}$. Consistently, as shown in Figures 8b, FG-6@Cur induced noticeably higher cell death in all Cur concentrations compared to the Free-Cur. The IC50 values of Free-Cur and FG-6@Cur were 292.68 µg $mL^{-1}$, 48.77 µg $mL^{-1}$ in PC-3 cells respectively, which is six-fold less than Free-Cur. These results confirm the curcumin intra-lysosomal release from FG-6@Cur, causing cancer cell apoptosis and its necrosis.

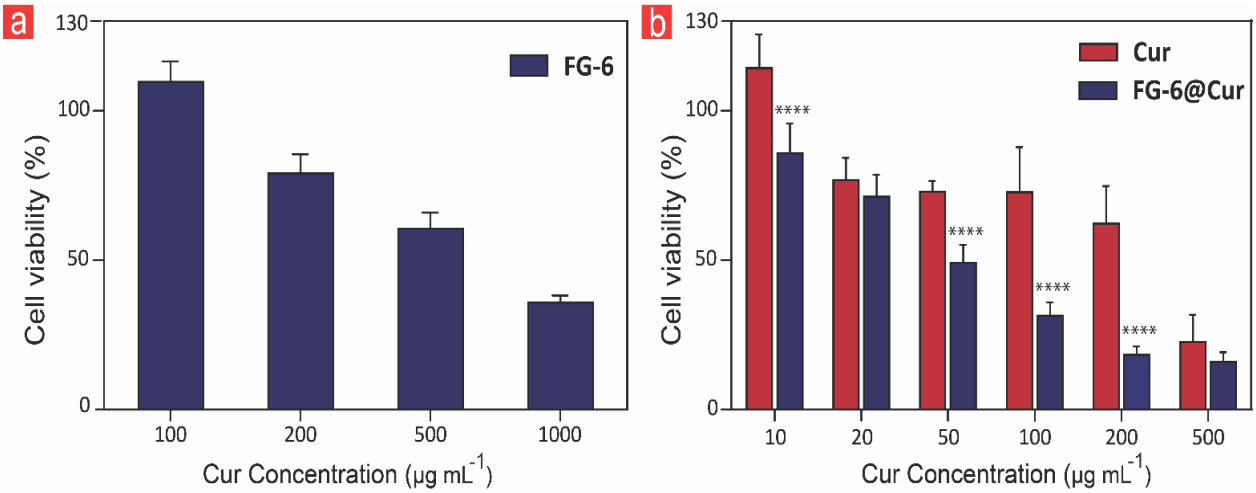


**Figure 8.** (a) Biocompatibility of FG-6 nanocarrier toward PC-3 cells after incubation for 24 h. (b) Viability of PC-3 cells treated with Cur and FG-6@Cur formulations at various Cur concentrations after incubation for 24 h. The results were expressed as mean ± SD based on six independent experiments and significant difference between groups appeared with *(P <0.05), **(P <0.01), ***(P <0.001) and ****(P <0.0001) using two-way ANOVA with Bonferroni's multiple comparisons test.

### 3.4. Intracellular uptake behavior

This study was conducted to evaluate intracellular uptake, and confocal laser scanning microscopy studied the curcumin distribution behavior of FG-6 nanocarriers to the nucleus, by PC-3 cell-lines. As shown in Figures 9a-b, inherent fluorescence properties of curcumin (red

color) were strong, and it was observed in the nuclei of cancer cells after 12h of treatment with FG-6@Cur. The results indicated an efficient curcumin distribution to the cancer cells nuclei.

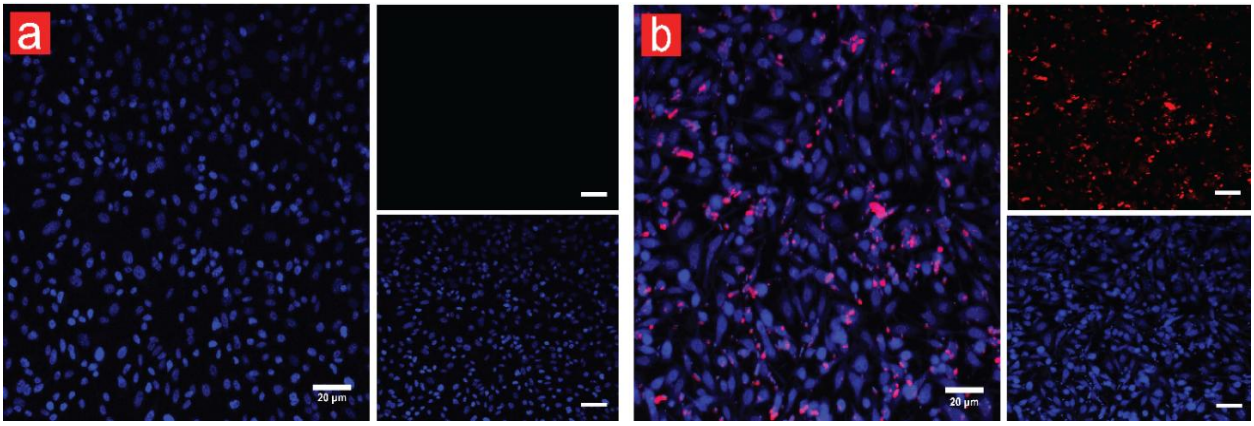


**Figure 9.** Confocal fluorescence images of PC-3 cell nuclei stained by DAPI dye and incubated with a fixed concentration of (a) Control and (b) FG-6@Cur (200 µg $mL^{-1}$) for 12h. Scale bar = 20 µm.

## 4. Conclusions

In summary, for the first time, we designed and fabricated a novel method to synthesize fluorinated graphene (FG) by using ionic liquid at a mild temperature (80 °C). We exploited a solid fluorine source ($NH_4F$) in the presence of a synthesized acidic ionic liquid and co-solvent (water/acetonitrile). This process was initiated by oxidizing the graphite and mild temperature fluorination by using an acidic ionic liquid. Of note, $[TEA]^+[TFA]^-$ as an acidic ionic liquid, was synthesized to have a catalysis role in fluorination of graphene oxide. More specifically, acidic ionic liquid allows larger protonation of hydroxyl and epoxide groups, which can subsequently increase the fluorination efficiently of this reaction. The obtained results proposed that the functional oxygen-containing groups in GO have an essential role in the FG formation process that by converting GO into the FG samples, the content of oxygen decreases considerably. The obtained FG of our procedure, among mild temperature methods, has maximum degree of fluorination (70.4 wt.% of F) and F/C ratio (2.4) as measured by XPS. Consequently, the

resulting FG nanosheets showed to have a higher Curcumin (a natural antitumor drug) loading efficiency when compared to that of FG that was purchased from industry. Most importantly, the Curcumin-loaded FG nanocarriers were successfully utilized to deliver the drug to the cancer cells nuclei and subsequently abrogating the. Overall, the proposed method for the preparation of FG is reported for the first time and has immense potential in the wide-ranging carbon-containing compounds for more extensive applications in numerous fields of research. Moreover, controlling various F/C ratios contribute to the bandgap energy alteration, unveiling potential applications of this method in optoelectronic and photonic devices.

**Acknowledgements**

The authors would like to acknowledge the Danish Council for Independent Research (Technology and Production Sciences, 5054–00142B).

**Conflicts of interest**

There are no conflicts to declare.

**Appendix A. Supplementary material**

The following are the supplementary data to this article:

Two figures related to experimental results: Figure S1. (a) 1H and (b) 13C NMR spectroscopy of ionic liquid ($[TEA]^{+}[TFA]^{-}$) and Figure S2. (a) Survey XPS spectra of Go, FG-1 and all FG that synthesized with different F/C ratios. (b) Tapping mode AFM topographic image of FG-6 nanosheets including the height profile and lateral width.

## References


[1] H. Zhang, Ultrathin Two-Dimensional Nanomaterials, ACS Nano. 9 (2015) 9451–9469. doi:10.1021/acsnano.5b05040.

[2] S. Talebian, M. Mehrali, N. Taebnia, C.P. Pennisi, F.B. Kadumudi, J. Foroughi, M. Hasany, M. Nikkhah, M. Akbari, G. Orive, A. Dolatshahi- Pirouz, Self- Healing Hydrogels: The Next Paradigm Shift in Tissue Engineering?, Adv. Sci. 6 (2019) 1801664. doi:10.1002/advs.201801664.

[3] V. Georgakilas, M. Otyepka, A.B. Bourlinos, V. Chandra, N. Kim, K.C. Kemp, P. Hobza, R. Zboril, K.S. Kim, Functionalization of Graphene: Covalent and Non-Covalent Approaches, Derivatives and Applications, Chem. Rev. 112 (2012) 6156–6214. doi:10.1021/cr3000412.

[4] W. Feng, P. Long, Y. Feng, Y. Li, Two-Dimensional Fluorinated Graphene: Synthesis, Structures, Properties and Applications, Adv. Sci. 3 (2016) 1500413. doi:10.1002/advs.201500413.

[5] Z. Yang, L. Wang, W. Sun, S. Li, T. Zhu, W. Liu, G. Liu, Superhydrophobic epoxy coating modified by fluorographene used for anti-corrosion and self-cleaning, Appl. Surf. Sci. 401 (2017) 146–155. doi:10.1016/j.apsusc.2017.01.009.

[6] Z. Wang, J. Wang, Z. Li, P. Gong, X. Liu, L. Zhang, J. Ren, H. Wang, S. Yang, Synthesis of fluorinated graphene with tunable degree of fluorination, Carbon N. Y. 50 (2012) 5403–5410. doi:10.1016/j.carbon.2012.07.026.

[7] M. Herraiz, M. Dubois, N. Batisse, S. Hajjar-Garreau, L. Simon, Large-scale synthesis of fluorinated graphene by rapid thermal exfoliation of highly fluorinated graphite, Dalt. Trans. 47 (2018) 4596–4606. doi:10.1039/C7DT04565D.

[8] P. Gong, Z. Yang, W. Hong, Z. Wang, K. Hou, J. Wang, S. Yang, To lose is to gain: Effective synthesis of water-soluble graphene fluoroxide quantum dots by sacrificing certain fluorine atoms from exfoliated fluorinated graphene, Carbon N. Y. 83 (2015) 152–161. doi:10.1016/j.carbon.2014.11.027.

[9] A. Mathkar, T.N. Narayanan, L.B. Alemany, P. Cox, P. Nguyen, G. Gao, P. Chang, R. Romero-Aburto, S.A. Mani, P.M. Ajayan, Synthesis of Fluorinated Graphene Oxide and its Amphiphobic Properties, Part. Part. Syst. Charact. 30 (2013) 266–272. doi:10.1002/ppsc.201200091.

[10] C. Sun, Y. Feng, Y. Li, C. Qin, Q. Zhang, W. Feng, Solvothermally exfoliated fluorographene for high-performance lithium primary batteries, Nanoscale. 6 (2014) 2634–2641. doi:10.1039/C3NR04609E.

[11] H. Chang, J. Cheng, X. Liu, J. Gao, M. Li, J. Li, X. Tao, F. Ding, Z. Zheng, Facile Synthesis of Wide-Bandgap Fluorinated Graphene Semiconductors, Chem. - A Eur. J. 17 (2011) 8896–8903. doi:10.1002/chem.201100699.

[12] G. Copetti, E.H. Nunes, G.V. Soares, C. Radtke, Mitigating graphene etching on SiO2 during fluorination by XeF2, Mater. Lett. 252 (2019) 11–14. doi:10.1016/j.matlet.2019.05.086.

[13] K. Fan, J. Fu, X. Liu, Y. Liu, W. Lai, X. Liu, X. Wang, Dependence of the fluorination intercalation of

graphene toward high-quality fluorinated graphene formation, Chem. Sci. 10 (2019) 5546–5555. doi:10.1039/C9SC00975B.

[14] H. Zhang, L. Fan, H. Dong, P. Zhang, K. Nie, J. Zhong, Y. Li, J. Guo, X. Sun, Spectroscopic Investigation of Plasma-Fluorinated Monolayer Graphene and Application for Gas Sensing, ACS Appl. Mater. Interfaces. 8 (2016) 8652–8661. doi:10.1021/acsami.5b11872.

[15] F. Gao, F. Liu, X. Bai, X. Xu, W. Kong, J. Liu, F. Lv, L. Long, Y. Yang, M. Li, Tuning the photoluminescence of graphene oxide quantum dots by photochemical fluorination, Carbon N. Y. 141 (2019) 331–338. doi:10.1016/j.carbon.2018.09.068.

[16] Z. Wang, J. Wang, Z. Li, P. Gong, X. Liu, L. Zhang, J. Ren, H. Wang, S. Yang, Synthesis of fluorinated graphene with tunable degree of fluorination, Carbon N. Y. 50 (2012) 5403–5410. doi:10.1016/j.carbon.2012.07.026.

[17] H. An, Y. Li, P. Long, Y. Gao, C. Qin, C. Cao, Y. Feng, W. Feng, Hydrothermal preparation of fluorinated graphene hydrogel for high-performance supercapacitors, J. Power Sources. 312 (2016) 146–155. doi:10.1016/j.jpowsour.2016.02.057.

[18] C. Min, Z. He, H. Song, H. Liang, D. Liu, C. Dong, W. Jia, Fluorinated graphene oxide nanosheet: A highly efficient water-based lubricated additive, Tribol. Int. 140 (2019) 105867. doi:10.1016/j.triboint.2019.105867.

[19] F.G. Zhao, G. Zhao, X.H. Liu, C.W. Ge, J.T. Wang, B.L. Li, Q.G. Wang, W.S. Li, Q.Y. Chen, Fluorinated graphene: Facile solution preparation and tailorable properties by fluorine-content tuning, J. Mater. Chem. A. 2 (2014) 8782–8789. doi:10.1039/c4ta00847b.

[20] H. Aguilar-Bolados, A. Contreras-Cid, M. Yazdani-Pedram, G. Acosta-Villavicencio, M. Flores, P. Fuentealba, A. Neira-Carrillo, R. Verdejo, M.A. López-Manchado, Synthesis of fluorinated graphene oxide by using an easy one-pot deoxyfluorination reaction, J. Colloid Interface Sci. 524 (2018) 219–226. doi:10.1016/j.jcis.2018.04.030.

[21] V. Mazánek, O. Jankovský, J. Luxa, D. Sedmidubský, Z. Janoušek, F. Šembera, M. Mikulics, Z. Sofer, Tuning of fluorine content in graphene: towards large-scale production of stoichiometric fluorographene, Nanoscale. 7 (2015) 13646–13655. doi:10.1039/C5NR03243A.

[22] O.Y. Posudievsky, A.S. Kondratyuk, O.A. Kozarenko, V.V. Cherepanov, G.I. Dovbeshko, V.G. Koshechko, V.D. Pokhodenko, Facile mechanochemical preparation of nitrogen and fluorine co-doped graphene and its electrocatalytic performance, Carbon N. Y. 152 (2019) 274–283. doi:10.1016/j.carbon.2019.06.031.

[23] L.E. Shmukler, M.S. Gruzdev, N.O. Kudryakova, Y.A. Fadeeva, A.M. Kolker, L.P. Safonova, Thermal behavior and electrochemistry of protic ionic liquids based on triethylamine with different acids, RSC Adv. 6 (2016) 109664–109671. doi:10.1039/C6RA21360J.

[24] E. Kowsari, A. Ehsani, M. Dashti Najafi, Electrosynthesis and pseudocapacitance performance of ionic liquid – Cr (η6-C6H5) complex functionalized reduced graphene oxide/poly ortho aminophenol nanocomposite film, J. Colloid Interface Sci. 504 (2017) 507–513. doi:10.1016/j.jcis.2017.05.117.

[25] N.P. Novoselov, E.S. Sashina, O.G. Kuz'mina, S. V. Troshenkova, Ionic liquids and their use for the

dissolution of natural polymers, Russ. J. Gen. Chem. 77 (2007) 1395–1405. doi:10.1134/S1070363207080178.

[26] A.R. Harifi-Mood, M. Aryafard, B. Minoofar, A. Ziyaei-Halimehjani, Specific spectroscopic behavior of Reichardt's betaine dye in binary mixtures of tetra-n-butylammonium glycinate and tetra-n-butylammonium l-alaninate with molecular solvents, J. Mol. Liq. 197 (2014) 315–321. doi:10.1016/j.molliq.2014.05.010.

[27] L. Kyllönen, A. Parviainen, S. Deb, M. Lawoko, M. Gorlov, I. Kilpeläinen, A.W.T. King, On the solubility of wood in non-derivatising ionic liquids, Green Chem. 15 (2013) 2374. doi:10.1039/c3gc41273c.

[28] A.S. Amarasekara, Acidic Ionic Liquids, Chem. Rev. 116 (2016) 6133–6183. doi:10.1021/acs.chemrev.5b00763.

[29] R.P. Swatloski, A.E. Visser, W.M. Reichert, G.A. Broker, L.M. Farina, J.D. Holbrey, R.D. Rogers, Solvation of 1-butyl-3-methylimidazolium hexafluorophosphate in aqueous ethanolâ€"a green solution for dissolving â€˜hydrophobicâ€™ ionic liquids, Chem. Commun. 1 (2001) 2070–2071. doi:10.1039/b106601n.

[30] K.R. Seddon, A. Stark, M.-J. Torres, Influence of chloride, water, and organic solvents on the physical properties of ionic liquids, Pure Appl. Chem. 72 (2000) 2275–2287. doi:10.1351/pac200072122275.

[31] D.C. Marcano, D. V. Kosynkin, J.M. Berlin, A. Sinitskii, Z. Sun, A. Slesarev, L.B. Alemany, W. Lu, J.M. Tour, Improved Synthesis of Graphene Oxide, ACS Nano. 4 (2010) 4806–4814. doi:10.1021/nn1006368.

[32] F. Chen, J. Zhang, L. Wang, Y. Wang, M. Chen, Tumor pH e -triggered charge-reversal and redox-responsive nanoparticles for docetaxel delivery in hepatocellular carcinoma treatment, Nanoscale. 7 (2015) 15763–15779. doi:10.1039/C5NR04612B.

[33] W. Huang, C.P. Tsui, C.Y. Tang, L. Gu, Effects of Compositional Tailoring on Drug Delivery Behaviours of Silica Xerogel/Polymer Core-shell Composite Nanoparticles, Sci. Rep. 8 (2018) 13002. doi:10.1038/s41598-018-31070-9.

[34] N. Kamaly, T. Kalber, M. Thanou, J.D. Bell, A.D. Miller, Folate Receptor Targeted Bimodal Liposomes for Tumor Magnetic Resonance Imaging, Bioconjug. Chem. 20 (2009) 648–655. doi:10.1021/bc8002259.

[35] D. Hu, Z. Xu, Z. Hu, B. Hu, M. Yang, L. Zhu, pH-Triggered Charge-Reversal Silk Sericin-Based Nanoparticles for Enhanced Cellular Uptake and Doxorubicin Delivery, ACS Sustain. Chem. Eng. 5 (2017) 1638–1647. doi:10.1021/acssuschemeng.6b02392.

[36] S. Han, Y. Liu, X. Nie, Q. Xu, F. Jiao, W. Li, Y. Zhao, Y. Wu, C. Chen, Efficient Delivery of Antitumor Drug to the Nuclei of Tumor Cells by Amphiphilic Biodegradable Poly(L-Aspartic Acid-co-Lactic Acid)/DPPE Co-Polymer Nanoparticles, Small. 8 (2012) 1596–1606. doi:10.1002/smll.201102280.

[37] S.-S. Han, Z.-Y. Li, J.-Y. Zhu, K. Han, Z.-Y. Zeng, W. Hong, W.-X. Li, H.-Z. Jia, Y. Liu, R.-X. Zhuo, X.-Z. Zhang, Dual-pH Sensitive Charge-Reversal Polypeptide Micelles for Tumor-Triggered Targeting Uptake and Nuclear Drug Delivery, Small. 11 (2015) 2543–2554. doi:10.1002/smll.201402865.

[38] K. Samanta, S. Some, Y. Kim, Y. Yoon, M. Min, S.M. Lee, Y. Park, H. Lee, Highly hydrophilic and insulating fluorinated reduced graphene oxide, Chem. Commun. 49 (2013) 8991–8993. doi:10.1039/c3cc45376f.

[39] W. Si, X. Wu, J. Zhou, F. Guo, S. Zhuo, H. Cui, W. Xing, Reduced graphene oxide aerogel with high-rate

supercapacitive performance in aqueous electrolytes, Nanoscale Res. Lett. 8 (2013) 247. doi:10.1186/1556-276x-8-247.

[40] P. Gong, J. Wang, K. Hou, Z. Yang, Z. Wang, Z. Liu, X. Han, S. Yang, Small but strong: The influence of fluorine atoms on formation and performance of graphene quantum dots using a gradient F-sacrifice strategy, Carbon N. Y. 112 (2017) 63–71. doi:10.1016/j.carbon.2016.10.091.

[41] R. Romero Aburto, L.B. Alemany, T.K. Weldeghiorghis, S. Ozden, Z. Peng, A. Lherbier, A.R. Botello Méndez, C.S. Tiwary, J. Taha-Tijerina, Z. Yan, M. Tabata, J.C. Charlier, J.M. Tour, P.M. Ajayan, Chemical Makeup and Hydrophilic Behavior of Graphene Oxide Nanoribbons after Low-Temperature Fluorination, ACS Nano. 9 (2015) 7009–7018. doi:10.1021/acsnano.5b01330.

[42] L. Chen, Z. Xu, J. Li, B. Zhou, M. Shan, Y. Li, L. Liu, B. Li, J. Niu, Modifying graphite oxide nanostructures in various media by high-energy irradiation, RSC Adv. 4 (2014) 1025–1031. doi:10.1039/C3RA46203J.

[43] F.-G. Zhao, G. Zhao, X.-H. Liu, C.-W. Ge, J.-T. Wang, B.-L. Li, Q.-G. Wang, W.-S. Li, Q.-Y. Chen, Fluorinated graphene: facile solution preparation and tailorable properties by fluorine-content tuning, J. Mater. Chem. A. 2 (2014) 8782–8789. doi:10.1039/C4TA00847B.

[44] P. Gong, J. Wang, W. Sun, D. Wu, Z. Wang, Z. Fan, H. Wang, X. Han, S. Yang, Tunable photoluminescence and spectrum split from fluorinated to hydroxylated graphene, Nanoscale. 6 (2014) 3316. doi:10.1039/c3nr05725a.

[45] R. Romero-Aburto, T.N. Narayanan, Y. Nagaoka, T. Hasumura, T.M. Mitcham, T. Fukuda, P.J. Cox, R.R. Bouchard, T. Maekawa, D.S. Kumar, S. V. Torti, S.A. Mani, P.M. Ajayan, Fluorinated Graphene Oxide; a New Multimodal Material for Biological Applications, Adv. Mater. 25 (2013) 5632–5637. doi:10.1002/adma201301804.

[46] K. Muthoosamy, I.B. Abubakar, R.G. Bai, H.-S. Loh, S. Manickam, Exceedingly Higher co-loading of Curcumin and Paclitaxel onto Polymer-functionalized Reduced Graphene Oxide for Highly Potent Synergistic Anticancer Treatment, Sci. Rep. 6 (2016) 32808. doi:10.1038/srep32808.

## Graphical abstract

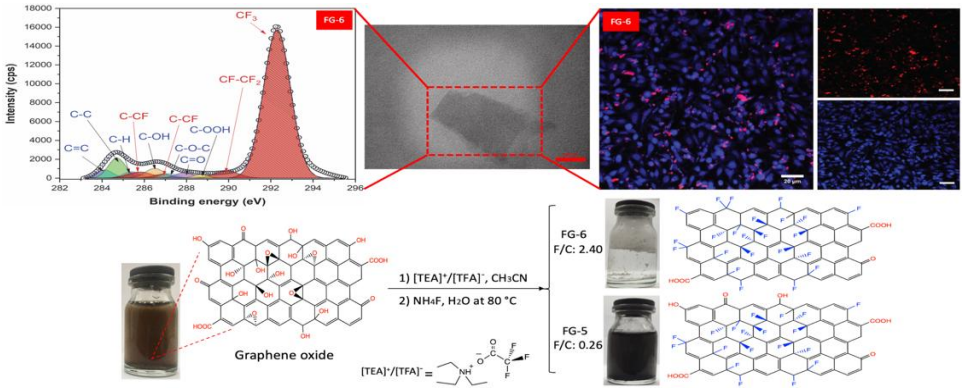

**Supplementary Material for on-line publication only**

**Click here to download Supplementary Material for on-line publication only: Supplementary data (1).docx**